The effect of natural organic matter on the adsorption of mercury to bacterial cells

Sarrah Dunham-Cheatham[1‡], Bhoopesh Mishra[2], Satish Myneni[3], and Jeremy B. Fein[1]

[1] *Department of Civil and Environmental Engineering and Earth Sciences, University of Notre Dame, Notre Dame, IN 46556, USA*
[2] *Department of Physics, Illinois Institute of Technology, Chicago, Illinois 60616, USA*
[3] *Department of Geosciences, Princeton University, Princeton, NJ 08544, USA*

Abstract

We investigated the ability of non-metabolizing *Bacillus subtilis*, *Shewanella oneidensis* MR-1, and *Geobacter sulfurreducens* bacterial species to adsorb mercury in the absence and presence of Suwanee River fulvic acid (FA). Bulk adsorption and X-ray absorption spectroscopy (XAS) experiments were conducted at three pH conditions, and the results indicate that the presence of FA decreases the extent of Hg adsorption to biomass under all of the pH conditions studied. Hg XAS results show that the presence of FA does not alter the binding environment of Hg adsorbed onto the biomass regardless of pH or FA concentration, indicating that ternary bacteria-Hg-FA complexes do not form to an appreciable extent under the experimental conditions, and that Hg binding on the bacteria is dominated by sulfhydryl binding. We used the experimental results to calculate apparent partition coefficients, K_d, for Hg under each experimental condition. The calculations yield similar coefficients for Hg onto each of the bacterial species studies, suggesting there is no significant difference in Hg partitioning between the three bacterial species. The calculations also indicate similar coefficients for Hg-bacteria and Hg-FA complexes. S XAS measurements confirm the presence of sulfhydryl sites on both the FA and bacterial cells, and demonstrate the presence of a wide range of S moieties on the FA in contrast to the bacterial biomass, whose S sites are dominated by thiols. Our results suggest that

‡ Corresponding author: dr.smdcheatham@gmail.com

© 2014. This manuscript version is made available under the Elsevier user license
http://www.elsevier.com/open-access/userlicense/1.0/

although FA can compete with bacterial binding sites for aqueous Hg, because of the relatively similar partition coefficients for the types of sorbents, the competition is not dominated by either bacteria or FA unless the concentration of one type of site greatly exceeds that of the other.

Introduction

Heavy metals, such as Hg, adsorb to proton-active functional groups on bacterial cell envelopes (e.g., Beveridge and Murray, 1976; Fortin and Beveridge, 1997; Daughney et al., 2002; Fein, 2006; Kenney and Fein, 2011), affecting the speciation and distribution of these metals in environmental systems. Recent studies (e.g., Guiné et al., 2006; Mishra et al. 2007; 2009; 2010; 2011; Joe-Wong et al., 2012; Pokrovsky et al., 2012; Song et al., 2012; Colombo et al., 2013; Yu et al., 2014) have shown that at least some bacterial cell envelopes contain proton-active sulfhydryl functional groups. Because Hg binds readily and strongly to sulfur compounds (Compeau and Bartha, 1987; Winfrey and Rudd, 1990; Benoit et al., 1999), bacterial adsorption of Hg may dramatically affect the distribution, transport and fate of Hg in geologic systems.

Natural organic matter (NOM) is present in nearly every near-surface geologic system, and complexation reactions between metals and NOM can dramatically change the behavior of the metals in the environment (McDowell, 2003; Ravichandran, 2004). NOM molecules contain a range of functional group types, including carboxyl, phenol, amino, and sulfhydryl groups, that have the potential to create highly stable complexes with metal ions across the pH scale (Ephraim, 1992; Ravichandran et al., 1999; Drexel et al., 2002; Haitzer et al., 2002; Croué et al., 2003; Ravichandran, 2004). Hg binds strongly to the sulfhydryl groups present within the NOM structure (Dong et al., 2011; Muresan et al., 2011). The relative thermodynamic stabilities of Hg-NOM and Hg-bacteria complexes are not well known. Depending on these relative stabilities, the

formation of metal-NOM complexes may decrease adsorption of Hg to bacteria cell envelopes due to a competitive ligand effect, or under certain conditions may increase adsorption of Hg to bacteria due to ternary complexation with NOM. For example, investigating Pb, Cu, and Ni separately, Borrok et al. (2007) found that ternary metal-FA-bacteria complexes form, and that the importance of the complexes is strongly affected by pH. Conversely, Wightman and Fein (2001) found that the presence of NOM decreases the amount of Cd adsorbed to bacteria under mid- and high-pH conditions, and that the presence of Cd does not affect the adsorption of NOM to bacteria, suggesting that ternary complexes do not occur. No studies have been conducted to date to determine the effects of NOM on Hg binding to bacteria. However, because Hg forms strong complexes both with cell envelopes (Daughney et al., 2002; Mishra et al., 2011; Dunham-Cheatham et al., 2014) and NOM (Loux et al., 1998; Ravichandran, 2004; Skyllberg et al., 2006), it is likely that significant changes to Hg adsorption behavior occur in the presence of NOM.

In this study, we used bulk adsorption and Hg X-ray absorption spectroscopy (XAS) experiments, conducted as a function of pH and FA concentration, using intact non-metabolizing bacterial cells to study Hg binding onto three different bacterial species and to compare the ability of bacteria to adsorb mercury in the presence and absence of a fulvic acid (FA). We used the experimental results to calculate apparent partition coefficients, K_d, for Hg-bacteria and Hg-FA complexes. This study examined both Gram-positive and Gram-negative bacterial species in order to determine if cell envelope structure affects the binding reactions, and one species was a Hg methylator, which we examined in order to determine if the extent or nature of Hg binding onto that species differed from that exhibited by the non-methylators.

Methods

Experimental methods

Bacterial growth and washing procedure

Bacillus subtilis (a Gram-positive aerobic soil species) and *Shewanella oneidensis* MR-1 (a Gram-negative facultative anaerobic species) cells were cultured and prepared following the procedures outlined in Borrok et al. (2007). Briefly, cells were maintained on agar plates consisting of trypticase soy agar with 0.5% yeast extract added. Cells for all experiments were grown by first inoculating a test-tube containing 3 mL of trypticase soy broth with 0.5% yeast extract, and incubating it for 24 h at 32 ℃. The 3 mL bacterial suspension was then transferred to 1 L of trypticase soy broth with 0.5% yeast extract for another 24 h on an incubator shaker table at 32 ℃. Cells were pelleted by centrifugation at 8100 g for 5 min, and rinsed 5 times with 0.1 M $NaClO_4$.

Geobacter sulfurreducens (a Gram-negative species capable of Hg methylation) cells were cultured and prepared using a different procedure than detailed above. Cells were maintained in 50 mL of anaerobic freshwater basal media (ATCC 51573) at 32 ^{o}C (Lovely and Phillips, 1988). Cells for all experiments were grown by first inoculating an anaerobic serum bottle containing 50 mL of freshwater basal media, and incubating it for 5 days at 32 ^{o}C. Cells were pelleted by centrifugation at 8100 g for 5 minutes, and rinsed 5 times with 0.1 M $NaClO_4$ stripped of dissolved oxygen by bubbling a 85%/5%/10% $N_2/H_2/CO_2$ gas mixture through it for 30 minutes. After washing, each of the three types of bacteria was then pelleted by centrifugation at 8100 g for 60 minutes to remove excess water in order to determine the wet mass so that suspensions of known bacterial concentration could be created. All bacterial concentrations in this study are given in terms of gm wet biomass per liter. Bacterial cells were harvested during

stationary phase, and all adsorption experiments were performed under oxic, non-metabolizing, electron donor-free conditions.

Adsorption experiments

To prepare experiments, aqueous Hg, NOM, and suspended bacteria stock solutions were mixed in different proportions to achieve the desired final concentrations for each experiment. The experiments were conducted in sets with constant pH (at pH 4.0 ± 0.1, 6.0 ± 0.1, or 8.0 ± 0.3) and constant bacterial concentration (0.2 g bacteria L^{-1} in all cases) at three different FA concentrations (0, 25, or 50 mg L^{-1}), with Hg log molalities ranging from -6.30 to -5.00 (0.1 to 2.0 mg L^{-1}).

FA stock solutions were prepared in Teflon bottles by dissolving dried, powdered International Humic Substances Society Suwannee River FA Standard I in a 0.1 M $NaClO_4$ buffer solution to achieve the desired final FA concentration for each experiment. A known mass of wet biomass was then suspended in the FA stock solution, and the pH of the FA-bacteria parent solution was immediately adjusted to the experimental pH using 0.2 M HNO_3 and/or NaOH. To prepare experimental solutions, aliquots of the FA-bacteria parent solution were added gravimetrically to Teflon reaction vessels, followed by a small aliquot of commercially-supplied 1,000 mg L^{-1} Hg aqueous standard to achieve the desired final Hg concentration. The pH of each suspension was again adjusted immediately to the experimental pH. The vessels were placed on an end-over-end rotator to agitate the suspensions for the duration of the experiment (2 h for *B. subtilis* and *G. sulfurreducens* and 3 h for *S. oneidensis* MR-1, as determined by initial kinetics experiments (results not shown)). The pH of the suspensions was monitored and adjusted every 15 minutes throughout the duration of the experiment, except during the last 30

minutes, when the suspensions were undisturbed. At the completion of each experiment, the pH of the suspensions was measured and the experimental suspensions were centrifuged at 8100 g for 5 minutes. The aqueous phase was collected for Hg analysis by inductively-coupled plasma optical emission spectroscopy (ICP-OES), and the solid phase of some of the runs was collected for XAS analyses. Duplicate experiments were performed for each experimental condition.

ICP-OES measurements

ICP-OES standards were prepared gravimetrically by diluting a commercially-supplied 1,000 mg L^{-1} Hg aqueous standard with pH-adjusted 0, 25, or 50 mg L^{-1} FA stock solution made in 0.1 M $NaClO_4$ so that the pH, ionic strength, and FA concentration of the standards closely matched that of the samples. We found significant interference when standards and samples were not closely matched in this way. The log molality of the Hg standards ranged from -6.60 to -5.00. The standards and samples were all stored in Teflon containers and analyzed with a Perkin Elmer 2000DV ICP-OES at wavelength 253.652 nm within 1 day of collection. The set of standards was analyzed before and after all of the samples were analyzed, as well as after every 15 samples, to check for machine drift. Analytical uncertainty, as determined by repeat analyses of the standards, was ± 2.8% for the 0 mg L^{-1} FA samples, ± 7.7% for the 25 mg L^{-1} FA samples, and ± 9.5% for the 50 mg L^{-1} FA samples. Neither standards nor samples were acidified prior to analysis. FA concentration strongly affected system performance and signal strength, likely due to spectral interferences caused by the FA molecule. Abiotic control experiments were conducted under conditions identical to the biotic experiments except without biomass present to determine the extent of Hg loss due to adsorption onto the experimental apparatus as well as any

interference caused by the presence of FA during the ICP-OES analysis. The extent of Hg removal in these controls did not vary systematically with pH and was below 10% adsorption.

XAS measurements

Hg L_{III}-edge X-ray absorption near edge structure (XANES) and extended X-ray absorption fine-structure spectroscopy (EXAFS) measurements were performed at the MRCAT sector 10-ID beamline (Segre et al., 2000), Advanced Photon Source, at Argonne National Laboratory. The continuous-scanning mode of the undulator was used with a step size of 0.5 eV and an integration time of 0.1 sec per point to decrease the radiation exposure during a single scan. Additionally, measurements were made at different spots on the samples to further decrease the exposure time. Hg XAS measurements were collected as described in Mishra et al. (2011).

Cinnabar (red HgS) and mercuric acetate crystalline powder standards were measured and used to calibrate the theoretical calculations against experimental data. Data collected from the powder standards were analyzed to obtain the S02 parameter, where S02 is the value of the passive electron reduction factor used to account for many-body effects in EXAFS. By fixing the values of S and O atoms to 2 in the cinnabar and mercuric acetate standards, we obtained S02 values of 1.02 ± 0.05 and 0.98 ± 0.03, respectively. Hence, we chose to set the value of S02 = 1.0 for all samples. Fitting of the powder standards to their known crystallographic structures reproduced the spectral features in the entire fitting range (1.0–4.2 Å), and fitting parameters were in agreement with previously reported values (Mishra et al., 2011). Only the paths necessary to model the solid standards were used for fitting the solution standards and the unknown Hg samples.

Two Hg species, Hg-cysteine and Hg-acetate, were utilized as solution-phase standards for Hg XAS analyses. First, an aqueous Hg^{2+} standard was prepared from high-purity 5 mM Hg^{2+} in 5% HNO_3 and was then adjusted to pH 2.0 ± 0.1 for measurement by adding appropriate amounts of 5 M NaOH. A Hg-cysteine standard was prepared by adding cysteine to the aqueous Hg^{2+} standard to achieve a Hg:ligand ratio of 1:100. The pH of the Hg-cysteine standard was adjusted to 5.0 ± 0.1 by adding appropriate amounts of 1 M or 5 M NaOH. A Hg-acetate standard was prepared by adding mercuric acetate salt to milliQ water and adjusting the pH to 5.0 ± 0.1 by adding appropriate amounts of 1 M or 5 M NaOH.

Sulfur K-edge XANES spectra for biomass and FA samples were acquired at sector 9-BM of the Advanced Photon Source at Argonne National Laboratory using Lytle detector in fluorescence detection mode. At 9-BM, the signal from higher order harmonics was removed by detuning the monochromator to 70% of maximum beam flux at 2472.0 eV. Energy calibration was performed by setting the first peak in the spectrum of sodium thiosulfate salt ($Na_2S_2O_3$) to 2469.2 eV. XANES spectra were measured between 2450 and 2500 eV. Step sizes in the near-edge region (2467-2482 eV) were 0.08 eV, and 0.2 eV in pre- and post- edge regions, respectively. Samples were smeared on carbon tape and the data were collected under a He atmosphere.

For this study, sulfur species are divided into three main categories and referred to as reduced S (below 2472 eV), sulfoxide S (near 2473.5 eV), and oxidized S (above 2476.5 eV). Accordingly, three commercially-supplied (Sigma Aldrich) S standards, cysteine, dimethyl sulfoxide (DMSO), and sodium dodecyl sulfate (NaDS), were used to fingerprint S speciation. S standards were mixed with a dry powder of polyacrylic acid (PAA) to achieve a mixture containing ~1% total S by mass. To perform S XANES measurements, a thin layer of a PAA-S

standard mixture was smeared on a carbon tape. All standards were prepared within 12 hours of analysis.

To prepare Hg XAS samples, FA was reacted with Hg by diluting a commercially-supplied 1000 mg L^{-1} Hg standard with a pH-adjusted 50 mg L^{-1} FA stock solution prepared in 0.1 M $NaClO_4$. The log molalities of Hg investigated were -4.30 and -3.60 at both pH 4.00 ± 0.10 and 8.00 ± 0.10 for each Hg concentration. *S. oneidensis* MR-1 biomass was also reacted with Hg in the presence and absence of FA to ascertain possible effects of FA on the Hg binding environment on the bacterial cell envelopes. Biomass was collected from the experiments with a log molality of Hg of -5.30 , pH values of 4.00 ± 0.10 or 8.00 ± 0.10, and 50 mg L^{-1} FA. Samples were loaded into slotted plexiglas holders that were subsequently covered with Kapton tape with a Kapton film sandwiched in between the tape and plexiglass to avoid direct contact of the sample with the tape adhesive. Samples were refrigerated until data collection. All measurements were conducted within 48 hours of sample preparation.

The data were analyzed by using the methods described in the UWXAFS package (Stern et al., 1995). Energy calibration between different scans was maintained by measuring Hg/Sn amalgam on the reference chamber concurrently with the fluorescence measurements of the biomass-bound Hg samples (Harris et al., 2003). The inflection point of the Hg L_{III}-edge (12.284 KeV) was used for calibration. Data processing and fitting were done with the ATHENA and ARTEMIS programs (Ravel and Newville, 2005). The data range used for Fourier transformation of the *k*-space data was 2.0–9.5 $Å^{-1}$. The Hanning window function was used with dk = 1.0 $Å^{-1}$. Fitting of each spectrum was performed in *r*-space, at 1.2-3.2 Å, with multiple *k*-weighting (k^1, k^2, k^3) unless otherwise stated. Lower χ_v^2 (reduced chi square) was used as the criterion for inclusion of an additional shell in the shell-by-shell EXAFS fitting procedure.

Partition coefficient calculations

To compare the Hg binding behavior in the presence and absence of FA, we calculated the apparent partition coefficients, K_d, for each experimental condition. K_d values were calculated by plotting the concentration of adsorbed Hg (Hg lost from the experiment due to binding to bacterial cells and/or FA) on the y-axis and the concentration of Hg remaining in solution on the x-axis for each data point collected in the adsorption experiments, considering only data for one bacterial species, pH condition, and FA condition as a function of initial Hg concentration at a time. The following equation was then used to calculate the K_d values:

$$K_d = \frac{[\text{Hg}]\ \text{adsorbed}}{[\text{Hg}]\ \text{remaining in solution}} \quad (1)$$

where K_d is the partition coefficient and the square brackets represent concentrations in mol L^{-1}. A best-fit line (Figure S1) was calculated for the data and the line was forced through the intersection (0,0) because if no Hg is added to the experiment then there would be a concentration of 0 for the amount of Hg adsorbed and of 0 for the Hg remaining in solution. The slope of the best-fit line then represents the K_d value for the dataset. 2σ uncertainties associated with each K_d value were estimated by determining the range of best-fit line slopes that would envelope approximately 95% of the data between them for each dataset.

Results and Discussion

Adsorption experiments

Consistent with previous studies of Hg adsorption onto bacteria (Daughney et al., 2002; Dunham-Cheatham et al., 2014), we observed extensive adsorption of Hg onto the bacterial species studied in the absence of FA, with the extent of adsorption relatively independent of pH between pH 4 and 8 (Figure 1, top plots). For example, approximately 77% of the Hg in a 2 mg L^{-1} Hg solution adsorbs at pH 4 onto 0.2 g L^{-1} *S. oneidensis* MR-1, while approximately 75%

adsorbs at pH 8. The presence of FA significantly decreases the concentration of Hg that adsorbs onto cell envelopes of each of the bacterial species and at each of the pH conditions studied (Figure 1, middle and bottom plots). With 50 mg L^{-1} FA, the extent of adsorption at pH 4 decreases to 65%, and at pH 8 to 50%. T-tests were performed to determine the statistical significance of the effect of FA in each bacterial system under each pH condition, and was determined to be significant relative to 0 mg L^{-1} FA in all systems (average p-value = 0.02). Our experimental results also indicate that the three bacterial species studied here exhibit similar extents of Hg adsorption under each experimental condition, consistent with the observations from a number of previous studies (e.g. Cox et al., 1999; Yee and Fein, 2001; Borrok et al., 2005, Johnson et al., 2007). Our data suggest that as the concentration of FA increases, so does the concentration of Hg remaining in solution. These results indicate that FA competes with the bacterial cells for the adsorption of Hg, and that the adsorption of Hg to FA results in a competitive ligand effect. As a result, less Hg is available for adsorption to proton-active functional groups on the bacterial cell envelope, and less Hg is removed from solution. These results are not surprising, as FA molecules contain sulfhydryl groups within their structure and sulfhydryl groups bind strongly with Hg (Xia et al., 1999; Hesterberg et al., 2001; Drexel et al., 2002; Haitzer et al., 2002; 2003), leading to effective competition with bacterial cell envelopes which also contain proton-active sulfhydryl functional groups (Guiné et al., 2006; Mishra et al., 2007; 2009; 2010; 2011; Pokrovsky et al., 2012; Song et al., 2012; Colombo et al., 2013; Yu et al., 2014). In our experimental systems, total FA binding sites outnumber those present on the bacteria. For example, 50 mg L^{-1} FA corresponds to approximately 2.8 x 10^{-4} moles of sites L^{-1} (Borrok and Fein, 2004), while 0.2 g L^{-1} *B. subtilis* biomass contains 4.7 x 10^{-5} total moles of sites L^{-1}. At pH 8, 50 mg L^{-1} FA does diminish the extent of Hg adsorption, but only from

approximately 75% (with no FA present) to 50%. Although the total number of binding sites associated with FA is greater than the total number of binding sites associated with bacterial biomass, the concentration of high-affinity sites on FA is lower than on bacteria (Rao et al., 2014). Thus given equal site concentrations, bacterial binding of Hg would dominate the competition with FA due to the higher concentration of higher-affinity thiol binding sites.

The calculated K_d values, presented in Figure 2, for the three bacterial species are similar to each other and do not vary systematically between bacterial species. Additionally, the calculated K_d values for the 25 mg L^{-1} FA and 50 mg L^{-1} FA data are not significantly different under the same pH conditions. The calculated K_d values do change systematically with pH, with values decreasing with increasing pH when FA is present; the same trend is not observed in the absence of FA. When comparing the FA-free and FA-bearing systems for one bacterial species under the same pH conditions, the K_d value for the FA-free system is significantly higher than the FA-bearing system in a majority of cases studied. These results suggest that the addition of FA to the experimental system decreases the amount of Hg removed from the solution relative to the FA-free system. This general conclusion is supported by our S XANES data, which demonstrate that the FA contains a wide range of S moieties while the bacterial biomass is dominated by a single thiol-type S moiety.

Hg XANES and EXAFS

To probe the effect of FA on Hg binding mechanisms with bacterial biomass, we examined Hg-biomass binding at pH 4 and 8 in the presence and absence of a stoichiometric excess of FA (1 mg L^{-1} Hg and 50 mg L^{-1} FA) using Hg L_{III} edge XANES and EXAFS. For the XAS studies, *S. oneidensis* MR-1 was chosen to represent the bacterial species used in this study.

Figure 3 shows a comparison between Hg XANES for Hg bound : 1) to FA and to *S. oneidensis* MR-1 biomass at pH 4, 2) to *S. oneidensis* MR-1 biomass in the presence and absence of FA at pH 4, 3) to *S. oneidensis* MR-1 biomass in the presence and absence of FA at pH 8, and 4) to cysteine, and to acetate. Hg XANES data indicate that Hg is complexed with thiol groups in each of the Hg-biomass samples. Spectral features supporting this conclusion are the small pre-edge peak and the slight dip at 12300 eV in the Hg-biomass XANES data similar to that present in the Hg-cysteine data. This finding is consistent with a previous study which showed Hg binding with sulfhydryl groups on *B. subtilis* cell envelopes under similar experimental conditions (Mishra et al., 2011). To understand these subtle differences in XANES, a linear combination fitting of the first derivative of the Hg-FA XANES data was performed which resulted in contributions of approximately 90% from Hg-cysteine binding and approximately 10% from Hg-carboxyl binding (Figure 4a). The first derivative of the Hg-biomass XANES data matched the first derivative of the Hg-cysteine standard, confirming that all of the Hg in the biomass samples was bound to thiol sites. XANES spectra of Hg reacted with *S. oneidensis* MR-1 biomass in the presence and absence of FA at pH 4 and 8 are reproducible, confirming that the binding mechanism of Hg with *S. oneidensis* MR-1 biomass does not change appreciably in the presence of FA.

Hg EXAFS results are consistent with the Hg XANES results described above. Differences between the coordination environments of Hg-FA and Hg-biomass are more pronounced in the $k^2 \bullet \chi(k)$ EXAFS data (Figure 5) than in the XANES data. The low signal to noise ratio in the aqueous Hg-FA data does not allow for a meaningful Fourier Transform (FT) of the Hg-FA EXAFS data. EXAFS $k^2\chi(k)$ and FT data between FA-bearing and FA-free Hg-biomass samples are similar (Figure 5), validating the Hg XANES results. Figure 4b shows a

comparison between the FT Hg EXAFS data for Hg bound to *S. oneidensis* MR-1 biomass in the presence and absence of FA at both pH 4 and 8 and their corresponding EXAFS fits. EXAFS fitting parameters are shown in Table S1. It is worth pointing out that although the Hg-cysteine standard yielded a bond distance of 2.32 Å, the Hg-biomass samples at pH 4 and 8 both had a bond distance of 2.35 Å. This should not be considered a discrepancy because Hg-S distances can vary from 2.32 to 2.36 A for $Hg(SR)_2$ complexes (Manceau,and Nagy, 2008). Similarly, Hg-S distances can range from 2.40 to 2.51 A for $Hg(SR)_3$ complexes, and 2.50–2.61 A for $Hg(SR)_4$ complexes. It has also been shown that Hg-S distances for Hg complexed with bacterial biomass can range from 2.32 Å to 2.51 Å, depending on the Hg:biomass ratio and the species of bacteria (Mishra et al., 2014).

Taken together, the Hg XANES and EXAFS spectroscopic results indicate that Hg binds predominantly to the high-affinity thiol groups on bacterial cell envelopes in the presence and absence of FA. Hg binding mechanisms with the bacterial biomass do not change in the presence of FA, ruling out the possibility of the formation of ternary complexes under the conditions studied. Additionally, Hg XAS results show that pH does not affect the adsorption mechanism of Hg onto biomass in the presence of FA, which is consistent with the similar extent of Hg adsorption as a function of pH described above. However, it is important to note that Hg binding mechanisms with bacterial biomass may be affected by FA at high Hg loadings, where Hg is primarily bound to biomass via more abundant, lower-affinity carboxyl functional groups (Mishra et al., 2010). Hg XAS results suggest that sulfhydryl functional groups on *S. oneidensis* MR-1 cell envelopes out-compete sulfhydryl functional groups in FA for Hg binding. In other words, on average Hg binding to FA appears weaker than Hg binding to bacterial biomass.

S XANES spectroscopy was conducted to identify the differences in complexation behavior of Hg with S functional groups on FA and bacterial biomass. S K-edge XANES is highly sensitive to changes in the electronic environment of the sulfur absorber (Xia et al., 1998). Although S K-edge XANES spectra were collected on a large number of standards, in this study we have divided S species into three main categories: reduced S (below 2472 eV), sulfoxide S (near 2473.5 eV), and oxidized S (above 2476.5 eV). The S XANES spectra for cysteine, dimethyl sulfoxide (DMSO), and sodium dodecyl sulfate (NaDS) are shown in Figure 6a. Species with very different S oxidation states, such as cysteine, sulfoxide, and ester sulfate, are easily resolved in the XANES spectrum. However, resolving one species from another within these three energy ranges is challenging. Reduced S species, including thiols, sulfides, polysulfides, and thiophenes give white-line features occurring between 2469 and 2472 eV. More extensive model libraries that include XANES spectra of organic and inorganic S compounds are available in the literature (Myneni, 2002; Vairavamurthy, 1998).

Speciation of S in the *S. oneidensis* MR-1 biomass was easily identified because the peak energy position of the S XANES measurement on the biomass overlaps with the cysteine peak position (Figure 6b). Figure 6b shows the dramatic differences between the S XANES signals from the *S. oneidensis* MR-1 cells and from the Suwanee River FA sample. S XANES comparing FA with *S. oneidensis* MR-1 shows that nearly the entire S budget of the biomass is present as thiol groups, which are known to form strong bonds with Hg. However, FA has a range of reduced S (including reactive thiol) groups and a large fraction of oxidized S species, consistent with previous observations (Morra et al., 1997). Morra et al. (1997) suggest that a significant fraction of sulfur in Suwanee River FA is oxidized (in a +5 oxidation state), with smaller fractions in reduced forms. Similarly, Einsiedl et al. (2007) used S XANES to estimate

that soil FAs contain approximately 51% oxidized (S^{4+},S^{5+},S^{6+}) and 49% reduced (S^{1-},S^{0},S^{2+}) sulfur species. The reduced S species in these samples were dominated by thiols, thiophene and disulfide. Rao et al. (2014) quantified the concentration of thiol groups on a range of ligands, including Suwanee River natural organic matter (SR-NOM) and *G. sulfurreducens*-PCA, and they report a thiol concentration on SR-NOM of 0.07±0.01 μM for a SR-NOM suspension of 100 mg L^{-1}, and a concentration of thiol on *G. sulfurreducens*-PCA of 0.34±0.05 μM for a bacterial suspension of 10^{13} cells L^{-1}. However, there is some disagreement about the concentration of sulfhydryl sites within NOM and bacterial cell envelopes, and the values reported for thiol concentrations by Joe-Wong et al. (2012) and by Yu et al. (2014) are significantly higher than those reported by Rao et al. (2014). Using the values for thiol concentrations reported by Joe-Wong et al. (2012) to calculate the concentration of thiols on FA (<2 μM per 25 mg L^{-1} FA) and *B. subtilis* (23.68±2.11 μM per g cell) yields a thiol concentration of <4 μM on FA (under the 50 mg L^{-1} FA condition) and 4.7 μM on *B. subtilis* in our experiments. The experimental Hg concentration range of our experiments was 0.5 to 10 μM, suggesting that there are sufficient numbers of high-affinity thiol sites to bind all of the Hg under the low Hg concentration conditions studied, and that most of the Hg can be bound to thiol groups under the higher Hg concentration conditions studied. Any additional Hg adsorption beyond the combined total thiol concentrations from FA and bacterial biomass is caused by Hg binding onto the more abundant, lower-affinity functional groups. These calculations demonstrate that bacteria and NOM may exhibit roughly similar thiol site concentrations in environmental systems, so under low metal loading conditions, the speciation and distribution of metals bound to NOM or bacteria may be quite sensitive to their relative concentrations and to the specific make-up of thiol sites within

each sorbent. A detailed study of the reactivity and stability of Hg with FA and bacterial biomass thiol sites is beyond the scope of this study.

The experimental results presented here suggest that bacterial cell envelope functional groups and FA functional groups exhibit different binding affinities for Hg under the experimental conditions. Hg binding onto the bacterial cell envelopes is extensive, and although Hg binds strongly with FA, especially with the sulfhydryl groups present within FA (Xia et al., 1999; Hesterberg et al., 2001; Drexel et al., 2002; Haitzer et al., 2002; 2003), the presence of even up to 50 ppm FA with only 0.2 g (wet mass) L^{-1} of bacteria does not cause the speciation of Hg to be dominated by the FA. The results suggest that there is a possibility for competition between the bacterial and FA binding sites for the available Hg.

Conclusions

The results from this study show that the presence of FA decreases the extent of Hg adsorption onto three different bacterial species through competitive binding of the Hg. The presence of the FA does not change the binding environment of Hg on the bacteria, indicating a lack of ternary complexation between the Hg, the FA, and the bacteria under the conditions studied. The binding of Hg to both the bacteria and the FA under the experimental conditions is dominated by sulfhydryl binding to both ligands, and the similarities between the binding environments likely results in the competitive balance between them. We used the experimental results to calculate partition coefficients for the binding of Hg to bacteria and FA, which can be used to estimate the distribution and speciation of Hg in bacteria- and FA-bearing geologic systems under conditions comparable to our experimental conditions.

Acknowledgements

Funding for this research was provided by a U.S. Department of Energy, Subsurface Biogeochemistry Research (SBR) grant. The experiments and analyses were performed at the Center for Environmental Science & Technology, University of Notre Dame. XAS measurements were obtained at the MRCAT-10-ID Beamline at the Advanced Photon Source (APS), Argonne National Laboratory. BM was supported by the Argonne Subsurface Scientific Focus Area project, which is part of the SBR Program of the Office of Biological and Environmental Research (BER), U.S. DOE under contract DE-AC02-06CH11357.

Three helpful and thorough journal reviews and the comments by Associate Editor Owen Duckworth significantly improved this work and are appreciated.

Figures

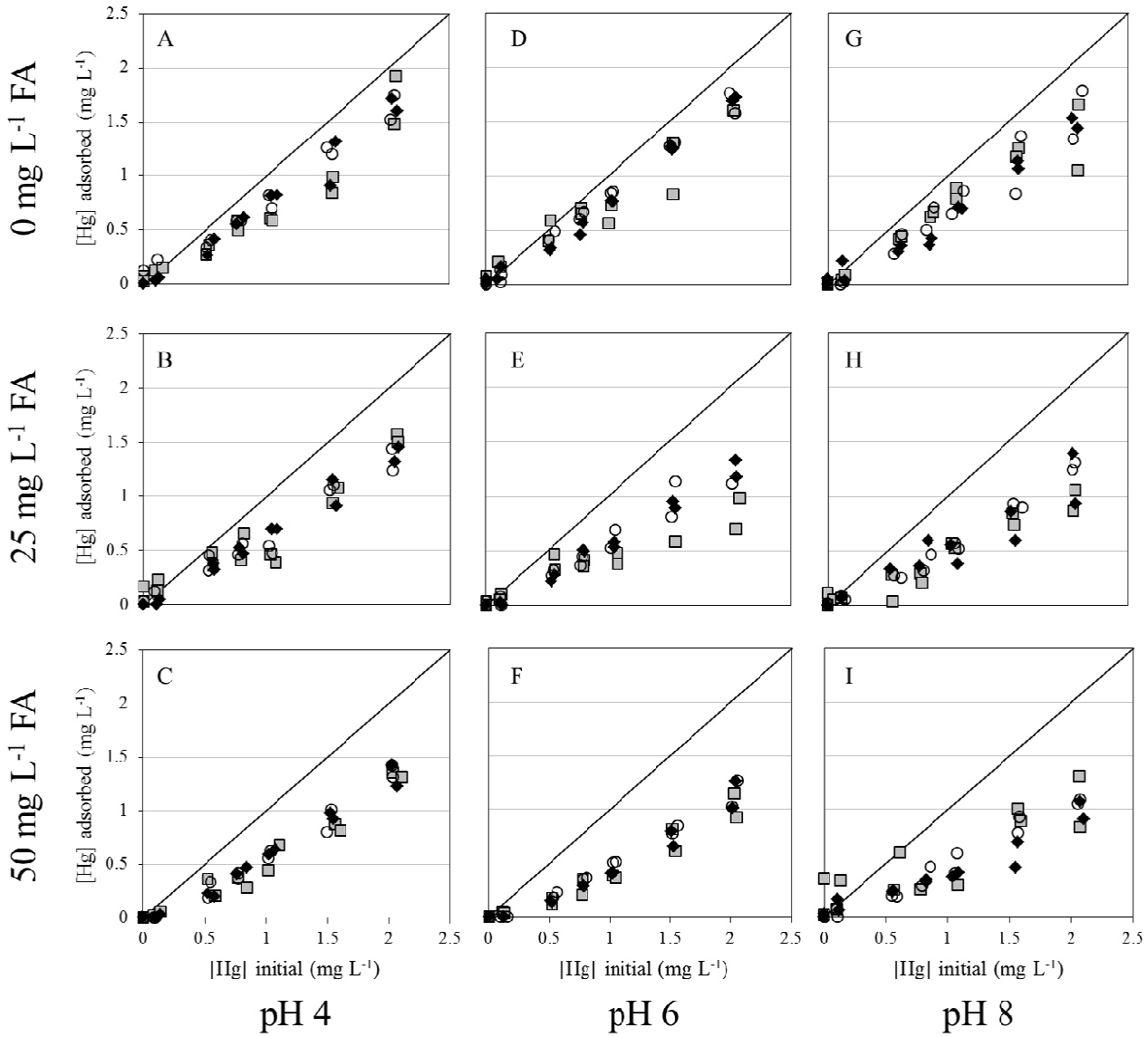

Figure 1: Aqueous chemistry results for Hg isotherms in the absence and presence of FA at pH 4 (A, B, C), pH 6 (D, E, F), and pH 8 (G, H, I). Plots A, D, and G present the results for the FA-free controls, plots B, E, and H present the results for the 25 mg L^{-1} FA experiments, and plots C, F, and I present the results of the 50 mg L^{-1} FA experiments. *B. subtilis* is represented by the black-outlined, grey-filled squares, *S. oneidensis* MR-1 is represented by the solid black diamonds, and *G. sulfurreducens* is represented by the hollow circles. The black line on each plot represents 100% Hg adsorption under each experimental condition.

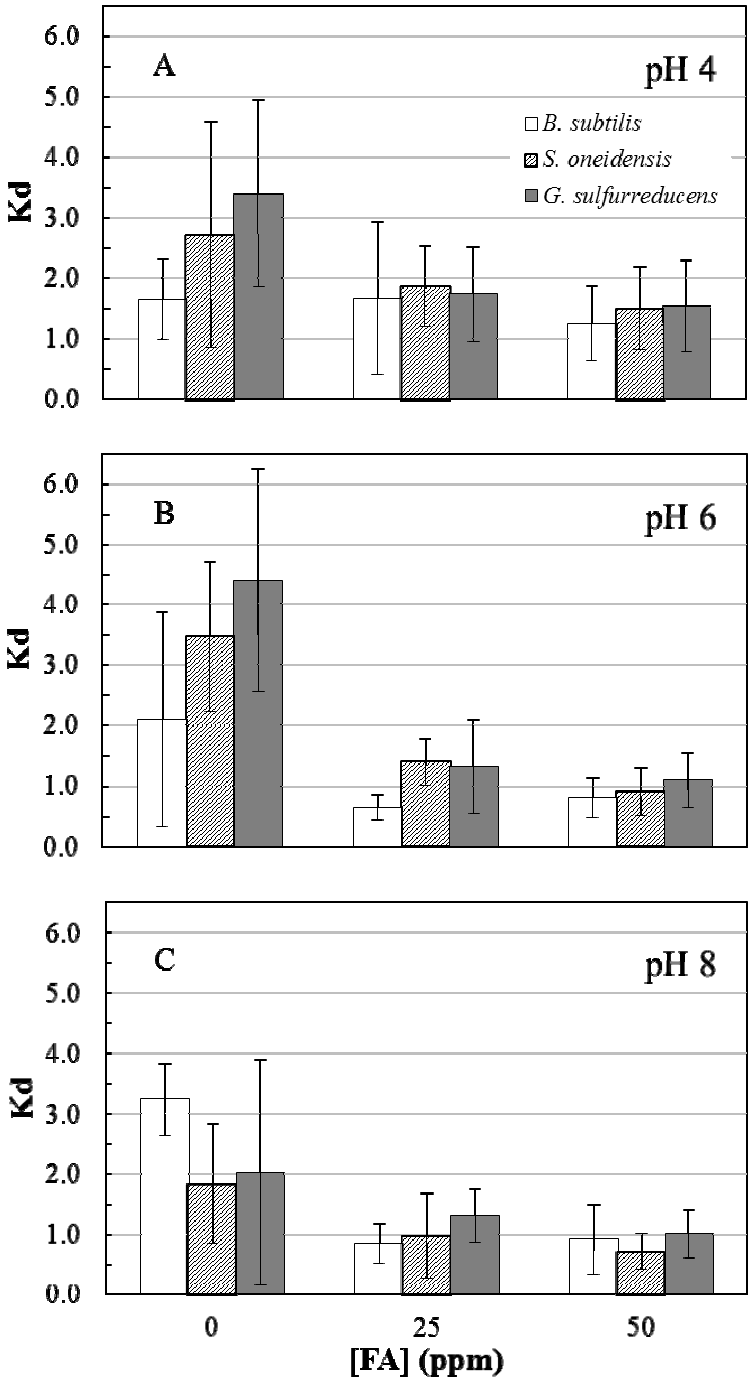

Figure 2: Calculated K_d values for all pH 4 (A), pH 6 (B), and pH 8 (C) fulvic acid conditions (on x-axis). *B. subtilis* is represented by the white bars, *S. oneidensis* MR-1 is represented by the hashed bars, and *G. sulfurreducens* is represented by the dark gray bars. Error bars represent 2σ.

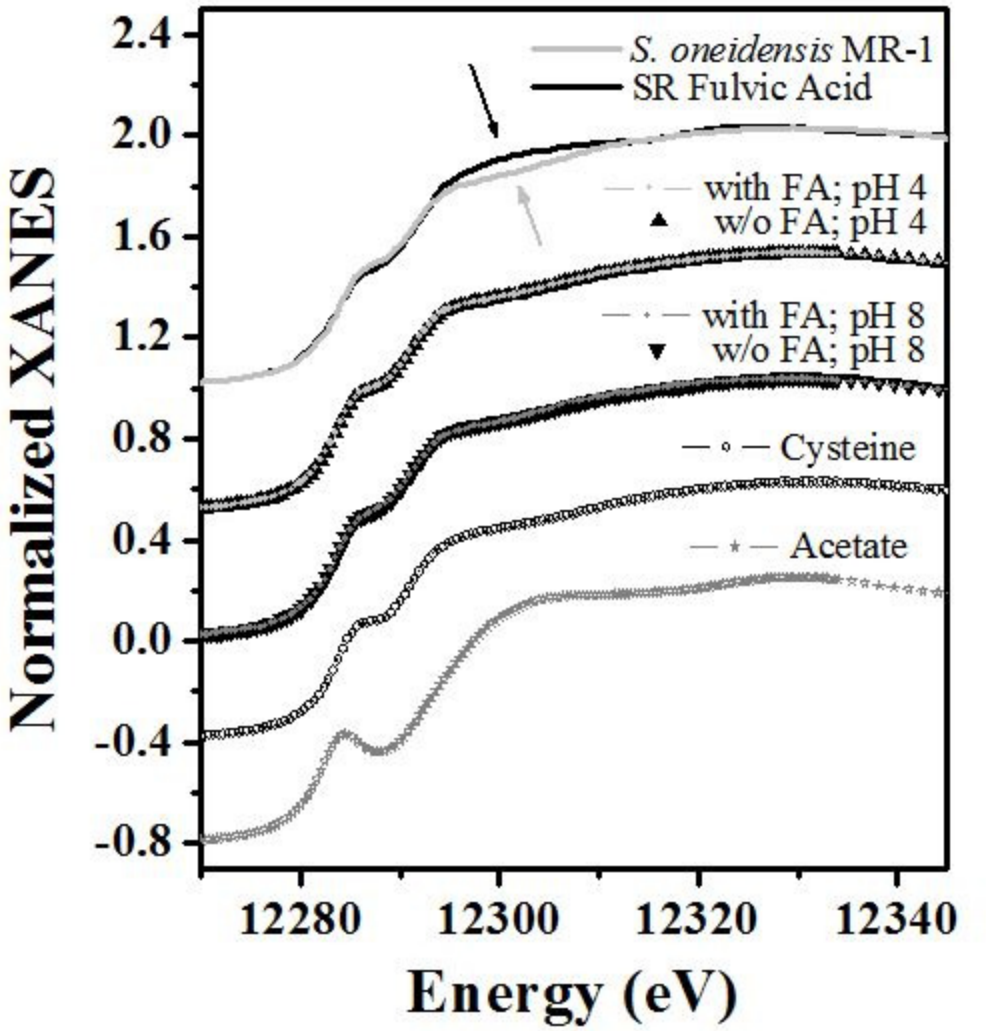

Figure 3: Hg L_{III} edge XANES spectra of Hg bound to (from top to bottom) *S. oneidensis* MR-1 only at pH 4, FA only at pH 4, *S. oneidensis* MR-1 in the presence of 50 and 0 mg L^{-1} FA at pH 4, *S. oneidensis* MR-1 in the presence of 50 and 0 mg L^{-1} FA at pH 8, cysteine only, and acetate only.

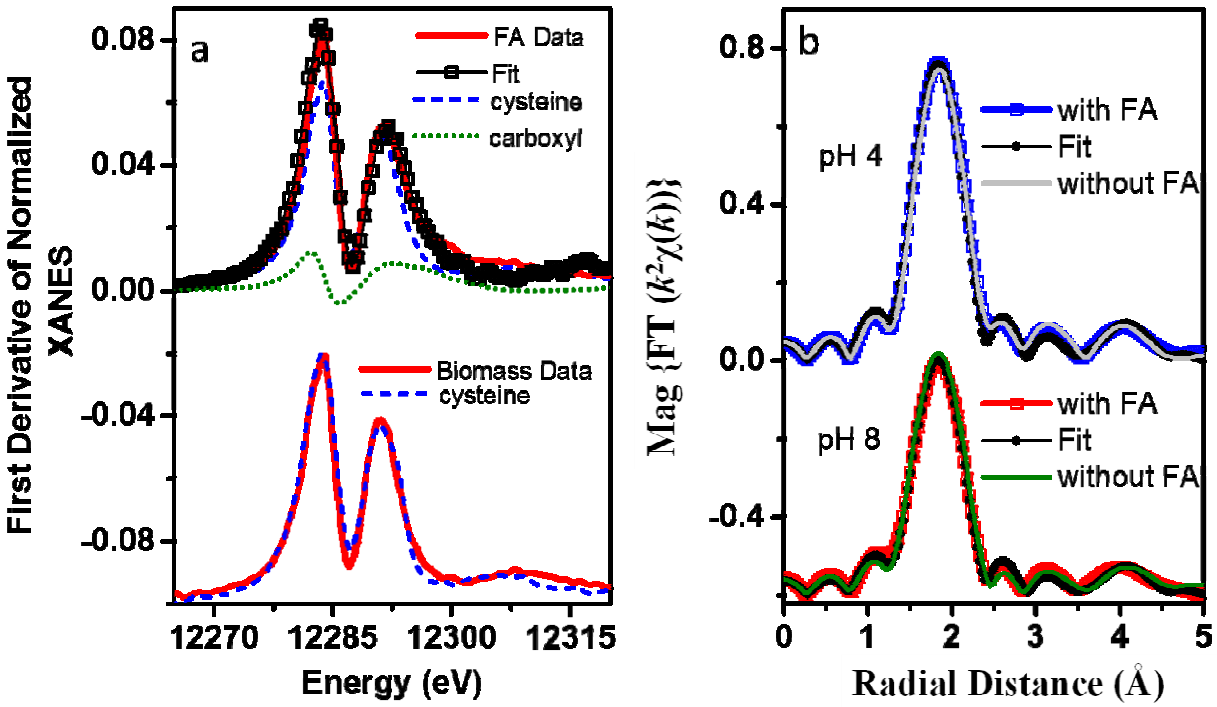

Figure 4: a) Linear combination fitting of the first derivative of the Hg-FA XANES data plotted with components. The first derivative of the Hg-biomass data is shown with the Hg-cysteine standard only. b) EXAFS Fourier transform (FT) data of the Hg-biomass data with and without fulvic acid at pH 4 and 8 overlaid with corresponding fits.

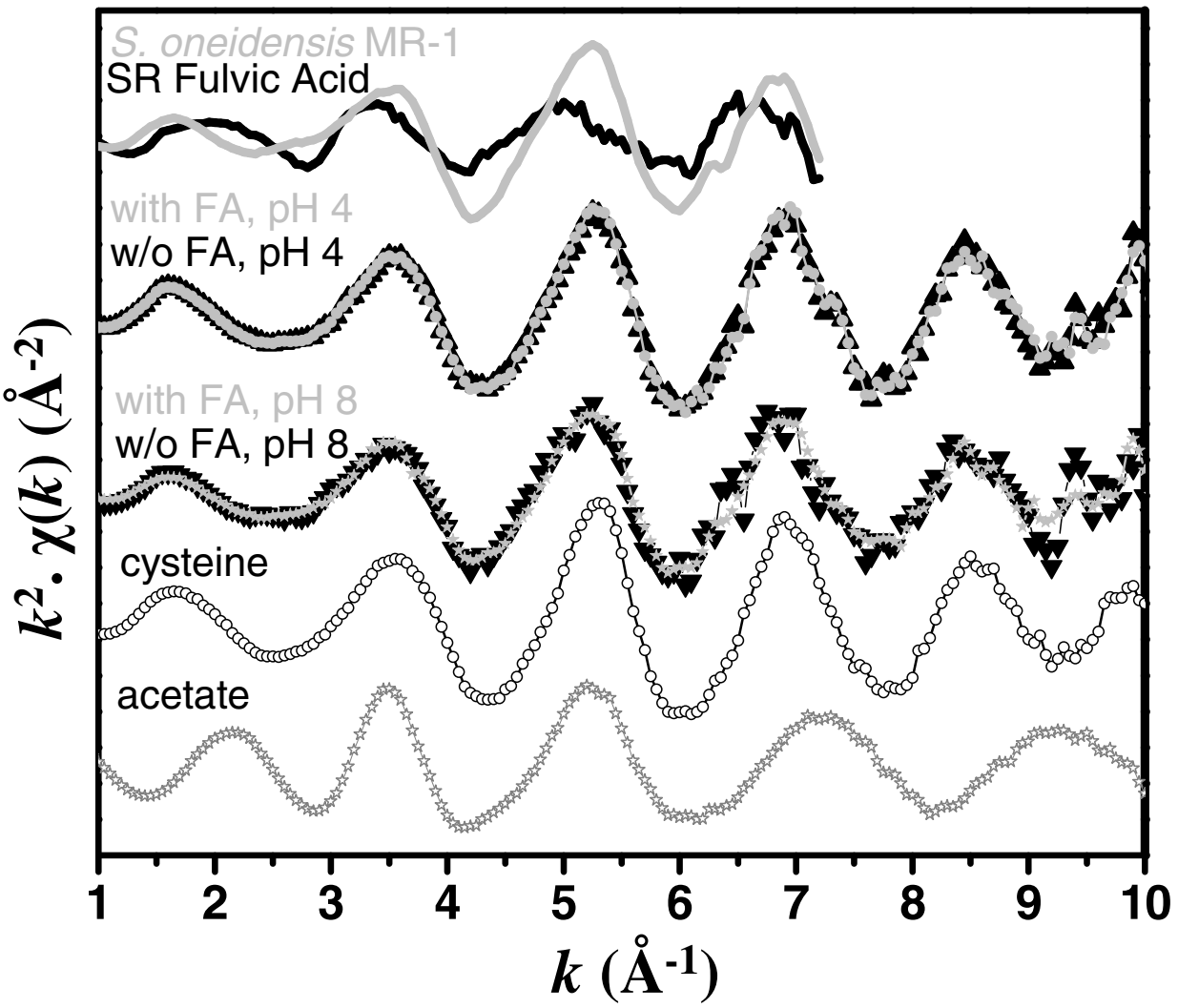

Figure 5: $k^2 \bullet \gamma(k)$ EXAFS data for Hg L_{III} edge EXAFS spectra of Hg bound to (top to bottom): *S. oneidensis* MR-1 only at pH 4, FA only at pH 4, *S. oneidensis* MR-1 in the presence of 50 and 0 mg L^{-1} FA at pH 4, *S. oneidensis* MR-1 in the presence of 50 and 0 mg L^{-1} FA at pH 8, cysteine only, and acetate only.

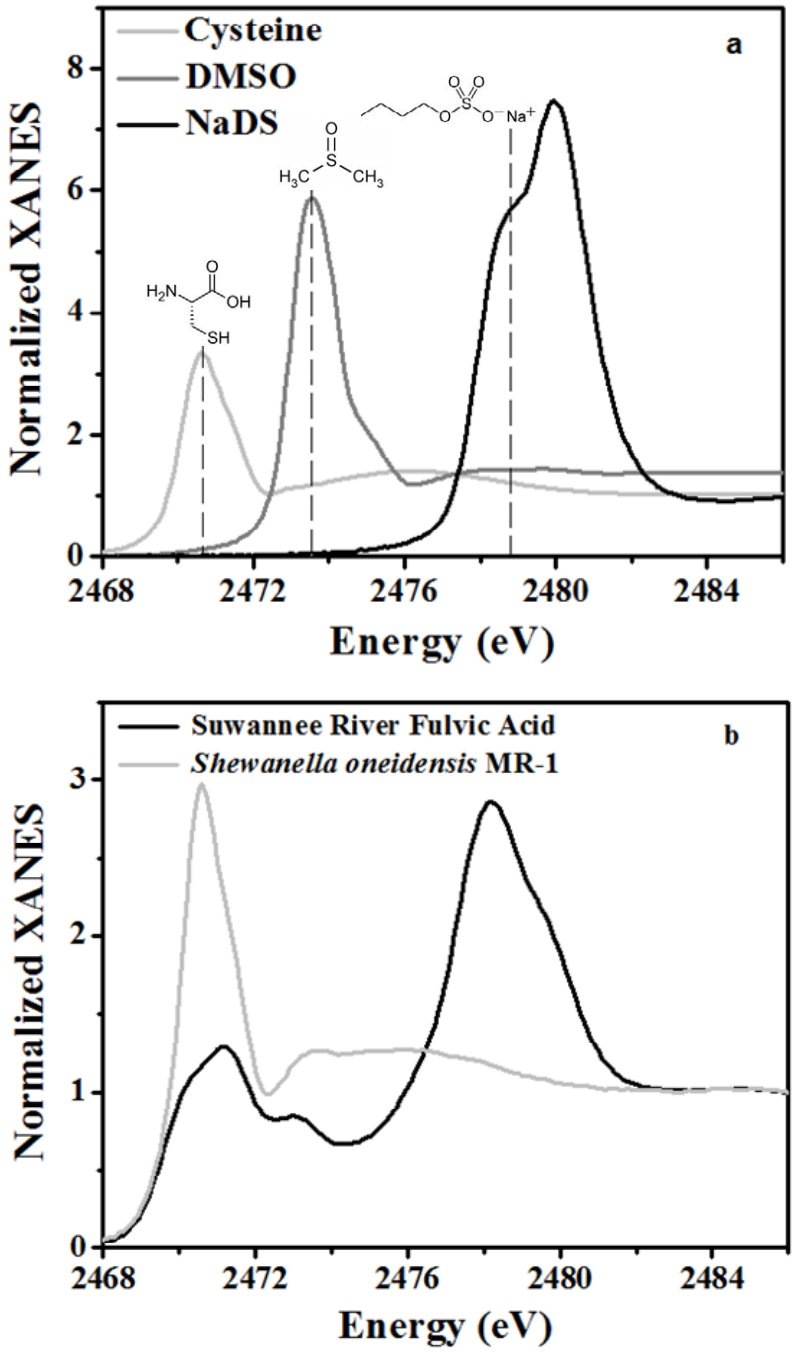

Figure 6: Sulfur K edge XANES spectra for a) cysteine, dimethyl sulfoxide (DMSO), and sodium dodecyl sulfate (NaDS), and b) *S. oneidensis* MR-1 biomass and Suwannee River FA.

References

Benoit J. M., Gilmour C. C., Mason R. P., and Heyes A. (1999) Sulfide Controls on Mercury Speciation and Bioavailability to Methylating Bacteria in Sediment Pore Waters. 33. 951-957.

Beveridge T. J., and Murray R. G. E. (1976) Uptake and retention of metals by cell walls of Bacillus subtilis. Journal of Bacteriology. 127. 1502-1518.

Borrok D and Fein J. B. (2004) Distribution of protons and Cd between bacterial surfaces and dissolved humic substances determined through chemical equilibrium modeling. Geochimica et Cosmochimica Acta. 68. 3043-3052.

Borrok D., Turner B. F., and Fein J. B. (2005) A universal surface complexation framework for modeling proton binding onto bacterial surfaces in geologic settings. American Journal of Science. 305. 826-853.

Borrok D., Aumend K. and Fein J. B. (2007) Significance of ternary bacteria-metal-natural organic matter complexes determined through experimentation and chemical equilibrium modeling. Chemical Geology. 238. 44-62.

Colombo M. J., Ha J., Reinfelder J. R., Barkay T., Yee N. (2013) Anaerobic oxidation of Hg(0) and methylmercury formation by *Desulfovibrio desulfuricans* ND132. Geochimica et Cosmochimica Acta. 112. 166-177.

Compeau G. C., and Bartha R. (1987) Effect of salinity on mercury-methylating activity of sulfate-reducing bacteria in estuarine sediments. Applied and Environmental Microbiology. 53. 261-265.

Cox J. S., Smith D. S., Warren L. A., and Ferris F. G. (1999) Characterizing heterogeneous bacterial surface functional groups using discrete affinity spectra for proton binding. Environmental Science & Technology. 33. 4514-4521.

Croué J.-P., Benedetti D., Violleau D., and Leenheer J. A. (2003) Characterization and Copper Binding of Humic and Nonhumic Organic Matter Isolated from the South Platte River: Evidence for the Presence of Nitrogenous Binding Sites. Environmental Science & Technology. 37. 328-336.

Daughney C. J., Siciliano S. D., Rencz A. N., Lean D., and Fortin D. (2002) Hg(II) adsorption by bacteria: A surface complexation model and its application to shallow acidic lakes and wetlands in Kejimkujik National Park, Nova Scotia, Canada. Environmental Science & Technology. 36. 1546-1553.

Dong W. M., Bian Y. R., Liang L. Y., and Gu B. H. (2011) Binding Constants of Mercury and Dissolved Organic Matter Determined by a Modified Ion Exchange Technique. Environmental Science & Technology. 45. 3576-3583.

Drexel R. T., Haitzer M., Ryan J. N., Aiken G. R., and Nagy K. L. (2002) Mercury(II) Sorption to Two Florida Everglades Peats: Evidence for Strong and Weak Binding and Competition by Dissolved Organic Matter Released from the Peat. Environmental Science & Technology. 36. 4058-4064.

Dunham-Cheatham S., Farrell B., Mishra B., Myneni S., and Fein J. B. (2014) The effect of chloride on the adsorption of Hg onto three bacterial species. Chemical Geology. 373. 106-114.

Einsiedl F., Hertkorn N., Wolf M., Frommberger M., Schmitt-Kopplin P., and Boris P. K. (2007) Rapid biotic molecular transformation of fulvic acids in a karst aquifer. Geochimica et Cosmochimica Acta. 71. 5474-5482.

Ephraim J. H. (1992) Heterogeneity as a concept in the interpretation of metal ion binding by humic substances. The binding of zinc by an aquatic fulvic acid. Analytica Chimica Acta. 267. 39-45.

Fein J. B., Boily J. F., Yee N., Gorman-Lewis D., and Turner B. F. (2005) Potentiometric titrations of Bacillus subtilis cells to low pH and a comparison of modeling approaches. Geochimica et Cosmochimica Acta. 69. 1123-1132.

Fein, J.B., 2006. Thermodynamic modeling of metal adsorption onto bacterial cell walls: current challenges. Adv. Agron. 90, 179–202.

Fortin D. and Beveridge T. J. (1997) Role of the bacterium Thiobacillus in the formation of silicates in acidic mine tailings. Chemical Geology. 141. 235-250.

Guiné V., Spadini L., Sarret G., Muris M., Delolme C., Gaudet J. P., and Martins J. M. F. (2006) Zinc sorption to three gram-negative bacteria: Combined titration, modeling, and EXAFS study. Environmental Science & Technology. 40. 1806-1813.

Haitzer M., Aiken G. R., and Ryan J. N. (2002) Binding of Mercury(II) to Dissolved Organic Matter: The Role of the Mercury-to-DOM Concentration Ratio. Environmental Science & Technology. 36. 3564-3570.

Haitzer M., Aiken G. R., and Ryan J. N. (2003) Binding of Mercury(II) to Aquatic Humic Substances: Influence of pH and Source of Humic Substances. Environmental Science & Technology. 37. 2436-2441.

Harris, H. H., Pickering, I. J., George, G. N. (2003) The Chemical Form of Mercury in Fish.Science. 301. 1203.

Hesterberg D., Chou J. W., Hutchison K. J., and Sayers D. E. (2001) Bonding of Hg(II) to Reduced Organic Sulfur in Humic Acid as Affected by S/Hg Ratio. Environmental Science & Technology. 35. 2741-2745.

Joe-Wong, C., Shoenfelt, E., Hauser, E.J., Crompton, N., Myneni, S.C.B. (2012) Estimation of reactive thiol concentrations in dissolved organic matter and bacterial cell membranes in aquatic systems. Environ. Sci. Technol. 46 (18), 9854–9861.

Johnson K. J., Szymanowski J. E. S., Borrok D., Huynh T. Q., and Fein J. B. (2007) Proton and metal adsorption onto bacterial consortia: Stability constants for metal-bacterial surface complexes. Chemical Geology. 239. 13-26.

Kenney J. P. L. and Fein J. B. (2011) Cell wall reactivity of acidophilic and alkaliphilic bacteria determined by potentiometric titrations and Cd adsorption experiments. Environmental Science & Technology. 45. 4446-4452.

Loux, N. T. (1998) An assessment of mercury-species-dependent binding with natural organic carbon. Chemical Speciation and Bioavailability. 10. 127-136.

Lovely, D.R. and Phillips, E.J.P. (1988) Novel mode of microbial energy metabolism: organic carbon oxidation coupled to dissimilatory reduction of iron or manganese. Applied and Environmental Microbiology. 54. 1472-1480.

Manceau A. and Nagy K. L. (2008) Relationships between Hg(II)-S bond distance and Hg(II) coordination in thiolates. Dalton Transactions. 11. 1421-1425.

Martell A. E. and Smith R. M. (2001) NIST Critically selected stability constants of metal complexes, Version 6.0. NIST Standard Reference Database. 46. National Institute of Standards and Technology. Gaithersburg, MD.

McDowell W. H. (2003) Dissolved organic matter in soils – future directions and unanswered questions. Geoderma. 113. 179-186.

Mishra, B., Fein, J. B., Boyanov, M. I., Kelly, S. D., Kemner, K. M., Bunker, B. A. (2007) Comparison of Cd Binding Mechanisms by Gram-Positive, Gram-Negative and Consortia of Bacteria Using XAFS. AIP Conference proceeding. 882. 343-345.

Mishra B., Boyanov M. I., Bunker B. A., Kelly S. D., Kemner K. M., Nerenberg R., Read-Daily B.L., and Fein J. B. (2009) An X-ray absorption spectroscopy study of Cd binding onto bacterial consortia. *Geochimica et Cosmochimica Acta.* 73. 4311-4325.

Mishra B., Boyanov M., Bunker B. A., Kelly S. D., Kemner K. M., and Fein J. B. (2010) High- and low-affinity binding sites for Cd on the bacterial cell walls of Bacillus subtilis and Shewanella oneidensis. *Geochimica et Cosmochimica Acta.* 74. 4219-4233.

Mishra B., O'Loughlin E. J., Boyanov M. B., Kemner K. M. (2011) Binding of HgII to High-Affinity Sites on Bacteria Inhibits Reduction to Hg^0 by Mixed $Fe^{II/III}$ Phases. Environmental Science & Technology. 45. 9597-9603.

Mishra B., Shoenfelt E., Yu Q., Yee N., Fein J. B., Myneni S.C.B. (2014) Mercury-thiol complexes on bacterial cell envelopes. Environmental Science and Technology Letters. (in revision)

Morra, M.J., Fendorf, S. E., Brown, P. D. (1997) Speciation of sulfur in humic and fulvic acids using X-ray absorption near-edge structure (XANES) spectroscopy. Geochimica et Cosmochimica Acta. 61. 683-688.

Muresan B., Pernet-Coudrier B., Cossa D., and Varrault G. (2011) Measurement and modeling of mercury complexation by dissolved organic matter isolates from freshwater and effluents of a major wastewater treatment plant. Applied Geochemistry. 26. 2057-2063.

Myneni, S. C. B. (2002) Soft X-ray spectroscopy and spectromicroscopy studies of organic molecules in the environment. Reviews in Mineralogy and Geochemistry. 49. 485-579.

Pokrovsky O.S., Pokrovski G. S., Shirokova L.S., Gonzalez A. G., Emnova E. E., Feurtet-Mazel A. (2012) Chemical and structural status of copper associated with oxygenic and anoxygenic phototrophs and heterotrophs: possible evolutionary consequences. Geobiology. 10. 130-149.

Powell K. J., Brown P. L., Byrne R. H., Gajda T., Hefter G., Sjoberg S., and Wanner H. (2005) Chemical speciation of environmentally significant heavy metals with inorganic ligands. Part

1: The Hg^{2+}-Cl^-, OH^-, CO_3^{2-}, SO_4^{2-}, and PO_4^{3-} aqueous systems. Pure and Applied Chemistry. 77. 739-800.

Rao, B., Simpson, C., Lin, H., Liang, L, and B. Gu. (2014) Determination of thiol functional groups on bacteria and natural organic matter in environmental systems. Talanta. 119. 240-247.

Ravel, B., Newville,M. (2005) ATHENA, ARTEMIS, HEPHAESTUS: Data analysis for X-ray absorption spectroscopy using IFEFFIT. Journal of Synchrotron Radiation. 12. 537–541.

Ravichandran M., Aiken G. R., Ryan J. N., and Reddy M. M. (1999) Inhibition of precipitation and aggregation of metacinnabar (mercuric sulfide) by dissolved organic matter isolated from the Florida Everglades. Environmental Science & Technology. 33. 1418-1423.

Ravichandran M. (2004) Interactions between mercury and dissolved organic matter – a review. Chemosphere. 55. 319-331.

Skyllberg U., Bloom P. R., Qian J., Lin C.-M., and Bleam W. F. (2006) Complexation of Mercury(II) in Soil Organic Matter: EXAFS Evidence for Linear Two-Coordination with Reduced Sulfur Groups. Environmental Science & Technology. 40. 4174-4180.

Segre, C. U., Leyarovsky, N. E., Chapman, L. D., Lavender, W. M., Plag, P. W., King, A. S., Kropf, A. J., Bunker, B. A., Kemner, K. M., Dutta, P., Duran, R. S., Kaduk, J. (2000) The MRCAT insertion device beamline at the Advanced Photon Source, CP521. Synchrotron Radiation Instrumentation: Eleventh U.S. National Conference; Pianetta, P., Ed.; American Institute of Physics:NewYork, 419–422.

Song Z., Kenney J. P. L., Fein J. B., Bunker B. A. (2012) An X-Ray Absorption Fine Structure study of Au adsorbed onto the non-metabolizing cells of two soil bacterial species. Geochimica et Cosmochimica Acta. 86. 103-117.

Stern, E. A., Newville, M., Ravel, B., Yacoby, Y., Haskel, D. (1995) The UWXAFS analysis package philosophy and details. Physica B. 209. 117–120.

Vairavamurthy, A. (1998) Using X-ray absorption to probe sulfur oxidation states in complex molecules. Spectrochimica Acta Part A: Molecular and Biomolecular Spectroscopy. 54. 2009-2017.

Westall J. C. (1982) FITEQL, A computer program for determination of chemical equilibrium constants from experimental data. Version 2.0. Report 82-02, Department of Chemistry, Oregon State University, Corvallis, OR, USA.

Wightman P. G. and Fein J. B. (2001) Ternary interactions in a humic acid-Cd-bacteria system. Chemical Geology. 180. 55-65.

Winfrey M. R. and Rudd J. W. M. (1990) Environmental factors affecting the formation of methylmercury in low pH lakes. Environmental Toxicology and Chemistry. 9. 853-869.

Xia K., Skyllberg U. L., Bleam W. F., Bloom P. R., Nater E. A., and Helmke P. A. (1999) X-ray Absorption Spectroscopic Evidence for the Complexation of Hg(II) by Reduced Sulfur in Soil Humic Substances. Environmental Science & Technology. 33. 257-261.

Xia K., Weesner, F., Bleam W.F., Helmke P.A., Bloom P.R., Skyllberg U.L. (1998) XANES Studies of Oxidation States of Sulfur in Aquatic and Soil Humic Substances. Soil Science Society of America Journal. 62. 124-1246.

Yee N. and Fein J. B. (2001) Cd adsorption onto bacterial surfaces: A universal adsorption edge? Geochimica et Cosmochimica Acta. 65. 2037.

Yu, Q., Szymanowski, J., Myneni S.C.B., and Fein, J.B. (2014) Characterization of sulfhydryl sites within bacterial cell envelopes using selective site-blocking and potentiometric titrations. Chemical Geology 373, 50-58.